

# Comparison of Psychro-active Arctic Marine Bacteria and Common Mesophilic Bacteria Using Surface-Enhanced Raman Spectroscopy

MARY L. LAUCKS, ATANU SENGUPTA, KAREN JUNGE, E. JAMES DAVIS, and BRIAN D. SWANSON\*

Department of Chemical Engineering, Box 351750, University of Washington, Seattle, Washington 98195-1750 (M.L.L., E.J.D.); Department of Chemistry, Box 351700, University of Washington, Seattle, Washington 98195-1700 (A.S.); and Department of Earth and Space Sciences, Box 351310, University of Washington, Seattle, Washington 98195-1310 (K.J., B.D.S.)

Psychro-active bacteria, important constituents of polar ecosystems, have a unique ability to remain active at temperatures below 0 °C, yet it is not known to what extent the composition of their outer cell surfaces aids in their low-temperature viability. In this study, aqueous suspensions of five strains of Arctic psychro-active marine bacteria (PAMB) (mostly sea-ice isolates), were characterized by surface-enhanced Raman spectroscopy (SERS) and compared with SERS spectra from *E. coli* and *P. aeruginosa*. We find the SERS spectra of the five psychro-active bacterial strains are similar within experimental reproducibility. However, these spectra are significantly different from the spectra of *P. aeruginosa* and *E. coli*. We find that the relative intensities of many of the common peaks show the largest differences reported so far for bacterial samples. An indication of a peak was found in the PAMB spectra that has been identified as characteristic of unsaturated fatty acids and suggests that the outer membranes of the PAMB may contain unsaturated fatty acids. We find that using suspensions of silver colloid particles greatly intensifies the Raman peaks and quenches the fluorescence from bacterial samples. This technique is useful for examination of specific biochemical differences among bacteria.

Index Headings: *Escherichia coli* bacteria; *Pseudomonas aeruginosa* bacteria; *Colwellia* bacteria; *Shewanella* bacteria; *Pseudoalteromonas* bacteria; Surface-enhanced Raman spectroscopy; SERS; Silver colloid particles; Psychro-active bacteria; Mesophilic bacteria.

## INTRODUCTION

In our previous study,<sup>1</sup> surface-enhanced Raman spectroscopy (SERS) was shown to be a potentially useful technique to characterize and distinguish certain strains of mesophilic (terrestrial or aquatic) bacteria (MTAB), bacteria that grow optimally at temperatures between 20 and 45 °C. In this paper we use SERS to study differences in bacterial outer-cell membrane structure by comparing the SERS spectra of two common MTAB strains, *Escherichia coli* and *Pseudomonas aeruginosa*, with 5 strains of psychro-active (including both psychrotolerant and psychrophilic) marine bacteria<sup>2-4</sup> (PAMB). Psychro-active bacteria are capable of growing at temperatures at least as low as -1 °C.

The five strains of PAMB are closely related to known marine psychrophiles of the genera *Shewanella*, *Pseudoalteromonas*, and *Colwellia*.<sup>5</sup> Sea-ice isolate 11B5 is closely related to *Shewanella frigidimara*, Arctic sediment isolate *Colwellia psychrerythraea* strain 34H (GenBank accession number: AF396670) and sea-ice iso-

late 6M3 both belong to the *Colwellia* genus, and the sea-ice isolates 6B1 and 6M4 are closely related to *Pseudoalteromonas antarctica*. The observed minimum temperature for growth of the strain 34H is -5 °C, but motility is maintained to -10 °C and this species is commonly found in sea ice.<sup>5-9</sup> The PAMB strains fall under the family Alteromonadaceae, order XI, Class 1 (Zylobacteria) of the  $\gamma$ -Proteobacteria, whereas *E. coli* and *P. aeruginosa* are in the same class, but in different orders, Enterobacteriales and Pseudomonadales, respectively.<sup>10</sup>

Psychro-active marine bacteria, typically found in polar regions,<sup>11,12</sup> have developed several strategies for survival in cold environments. Research to date has focused on the distribution of PAMB in sea-ice,<sup>13,14</sup> their biological diversity,<sup>2</sup> and their enzyme and membrane adaptations.<sup>4,7,15</sup> But the outer cell surface of the organisms, which directly interacts with and mediates between the organism and its environment, remains to be characterized chemically.

Much research on cold adaptation has focused on PAMB from Arctic or Antarctic marine habitats.<sup>7</sup> Since membrane flexibility decreases with temperature, much of the work on cold adaptation has attempted to correlate changes of fatty acid composition<sup>15-17</sup> with changes in salinity and optimal growth temperature. Results from these studies indicate that PAMB show an increase in unsaturated and branch-chained fatty acids and a decrease in the length of lipids. More recently, it was found that Antarctic PAMB produce polar carotenoids that decrease membrane fluidity at low temperatures.<sup>18,19</sup> Such carotenoids may act to counterbalance the effects of unsaturated fatty acids and fine-tune membrane fluidity. The production of polyunsaturated fatty acids (PUFAs) occurs in many PAMB including Antarctic sea-ice bacteria<sup>4</sup> and is particularly common within the genera of *Colwellia* and *Shewanella*.<sup>20</sup> However, *E. coli* and *P. aeruginosa* do not synthesize PUFAs, which suggests that different chemical or structural elements may be present in their cell membranes.

Surface-enhanced Raman scattering (SERS) (first observed by Fleischmann in 1974)<sup>21</sup> is useful for studying biological materials and single molecules<sup>22</sup> because the signal is typically many orders of magnitude more intense than ordinary Raman scattering and quenches the fluorescence of biological molecules.<sup>1</sup> SERS requires the presence of metal atoms in close proximity to the molecule of interest (the analyte). It has been shown that large enhancements in signal can be obtained when, instead of

Received 22 March 2005; accepted 9 August 2005.

\* Author to whom correspondence should be sent. E-mail: brian@ess.washington.edu.

a solid metal surface, either a specially prepared metal film, a suspension of colloidal metal particles (Ag, Au, or Cu),<sup>23</sup> or carbon nanotubes<sup>24</sup> with certain regular nano-scale structures are used.

The size of the colloidal particles or film structures may determine which molecular bonds are enhanced,<sup>25</sup> but the typical colloid particle size is in the range 10–100 nm. The magnitude of the enhancement is also determined by whether the colloidal particles cover the analyte (if the analyte is a cell or other large biological complex) or if the analyte covers the colloidal particles (if the analyte is of molecular size).<sup>1</sup> There is an excellent review of the SERS technique by Moscovits.<sup>26</sup>

There have been many recent SERS studies characterizing the spectra of various single cells, spores, DNA, amino acids, peptides, and proteins.<sup>27–33</sup> Recent SERS studies of bacteria,<sup>1,34,35,40</sup> have attempted to distinguish or “fingerprint” bacteria. Zeiri et al.<sup>34</sup> did not observe large differences between the spectra of the gram-negative and gram-positive bacteria they studied. On the other hand, Jarvis and Goodacre<sup>35</sup> found that with discriminant function analysis (DFA), hierarchical cluster analysis (HCA), and some *a priori* knowledge about class differences, they could clearly distinguish between their bacterial samples.

It is well known that the preparation and handling of colloid suspensions of silver affects the resultant SERS spectra from analyte adsorbed on the colloid particles (see references cited within Keir et al.<sup>36</sup>). Munro et al.<sup>37</sup> report on an optimization study of a citrate-reduced colloid (following a procedure reported by Lee and Meisel).<sup>38</sup> They find that the citrate-reduction method is more stable and reproducible, as measured by visible absorption spectra, than the borohydride-reduction method used in this study. In addition, they find that the magnitude of the SERS enhancement for the citrate-reduced colloids is greater.

However, we found from the literature that the citrate-reduction method was much less reproducible in the laboratory than the borohydride-reduction method of Keir et al.,<sup>39</sup> so we chose to use the latter for making our colloidal suspensions.

Using the borohydride-reduction method, Sengupta et al.<sup>1</sup> found that the variations between samples of the same bacteria can be as large as those between different bacterial samples unless certain variables are carefully controlled: volume ratio (bacterial to colloidal suspension), age of colloid, time after mixing bacteria and colloid, and colloidal preparation. However, when these variables are controlled it was found that small differences could be observed between various bacterial strains over certain ranges of Raman shift ( $\text{cm}^{-1}$ ), without DFA. Moreover, when three pollen families were compared, Sengupta et al.<sup>40</sup> found that the SERS spectra of the pollen families are significantly different.

## EXPERIMENTAL

The SERS spectra shown in this paper were obtained using a bioanalyte/silver colloid mixture. The silver colloidal suspensions of  $10^{-4}$  M concentration were made using the method of Keir et al.<sup>39</sup> The PAMB were mixed with the  $10^{-4}$  M Ag colloid in a volume ratio of 100:1

(Ag colloid solution to aqueous bacterial suspension). The bacterial suspensions were prepared up to one day (24 h) before being mixed with the colloid solution, and most Raman spectra were obtained within 20 min after the bacterial/colloidal mixture was prepared. The bacteria solutions were stored between data runs in a refrigerator at 4–6 °C. The MTAB spectra were acquired in 60 s and the PAMB spectra were acquired in 300 and 400 s.

The spectra were obtained using an argon-ion laser at a wavelength of 514.5 nm and 100 mW of laser light incident onto the sample. The spectrum of the scattered light was analyzed by a 500-mm focal-length single-pass Acton SpectraPro-500i spectrometer after attenuation of the laser line by a Kaiser Optical Systems SuperNotch-Plus holographic filter. The detector was a Princeton Instruments back-illuminated, liquid-nitrogen-cooled  $1340 \times 100$  pixel array charge-coupled device (CCD) camera.

Cultures of *E. coli* and *P. aeruginosa* were grown for 15–20 h in Luria broth, centrifuged, and washed twice before being re-suspended in 2 mL of deionized water. The optical density of the bacterial suspensions, *E. coli* and *P. aeruginosa*, ranges from 0.5 to 3.4 and gives an indication of bacterial concentration. These bacterial suspensions were mixed in various ratios with the silver colloid solution. We found that for *E. coli* and *P. aeruginosa* grown to the stationary stage our optimal volume ratio (for the best spectra) was 50 parts silver colloid solution to 1 part bacterial suspension. Additional experimental details are described in a previous paper.<sup>1</sup>

The Arctic sea-ice bacterial strains 11B5, 6B1, 6M4, and 6M3 were isolated from ice-core samples collected during the Arctic West Summer 1996 (AWS96) cruise of the USCGC icebreaker “Polar Sea” into the Chukchi Sea.<sup>5</sup> *C. psychrerythraea* strain 34H was isolated from Arctic shelf sediments.<sup>6</sup> Cultures of 34H, 11B5, 6B1, 6M4, and 6M3 were grown at  $-1$  °C for 14 days (to late exponential growth) in half-strength Marine 2216 broth (DIFCO laboratories, Detroit, MI). Bacterial cells in 5 mL of the culture medium were centrifuged at 3000 rpm for 10 min, washed twice in artificial seawater (for 1 L of solution: 24 g NaCl, 0.7 g KCl, 5.3 g  $\text{MgCl}_2 \cdot 6\text{H}_2\text{O}$ , 7.0 g  $\text{MgSO}_4 \cdot 7\text{H}_2\text{O}$ , and 1.3 g TAPSO buffer), and after the final centrifugation step were re-suspended into 2.5 mL artificial seawater. The resulting bacterial suspensions were found to have an optical density between 0.5 and 1.5.

## RESULTS AND DISCUSSION

***E. coli* and *P. aeruginosa* Spectra.** The *E. coli*/silver colloid (Volume ratio, VR = 50:1) spectrum shown in Fig. 1 is the average of three spectra normalized to the  $1635 \text{ cm}^{-1}$  water peak to adjust for background differences. To obtain the normalized average spectra, the steps were as follows: (1) divide each intensity (all three spectra) by the integration time to get counts per second, (2) multiply each of these values by a factor that normalizes to the height of the water peak of one spectrum, (3) shift the spectra so that the water peaks overlap, and (4) take the average of all three spectra. The dominant peak is at  $1355 \text{ cm}^{-1}$ , and other major peaks occur at 1635, 1587, 1539, 1460, 1283, 1240, 1166, 956, 813, 753, 703, 636, and  $571 \text{ cm}^{-1}$ .

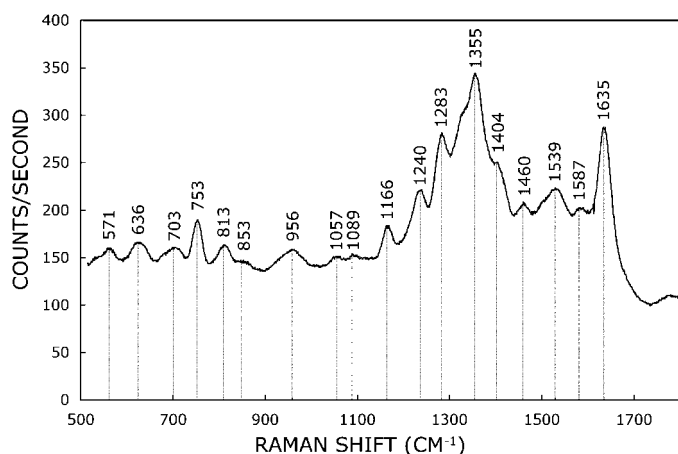


Fig. 1. Average of three *E. coli* spectra. The lines are positioned on the major peaks that appear in Table I. The VR was 50:1 (Ag colloid to bacterial suspension).

We also investigated a different method of analysis: instead of normalizing to the height of the water peak at  $1635\text{ cm}^{-1}$ , we subtracted a pure deionized water spectrum (first normalized to the background intensity of the *E. coli* spectrum) from each of the *E. coli* spectra, since the MTAB were all suspended in deionized water. The steps were as follows: (1) divide each bacterial spectrum by the integration time, (2) subtract background value at  $1827\text{ cm}^{-1}$  from all data points, (3) subtract background at  $1827\text{ cm}^{-1}$  from all points of the deionized water (after having converted to counts per second), and (4) subtract the resulting deionized water spectra point by point from the *E. coli* spectra. Comparing the results of the two methods, it is clear that, for high signal-to-noise ratio spectra, the water background is a very small fraction of the overall intensity, so that the two methods produce almost identical results. However, for small signal-to-noise spectra, such as the PAMB spectra, the results are significantly different for the two methods. As will be explained below, we chose to analyze the PAMB spectra by first subtracting the artificial seawater background.

Figure 2 shows 24 spectra from suspensions of *P. aeruginosa*/silver colloid (VR = 50:1). The dominant peak occurs at  $1354\text{ cm}^{-1}$  and other major peaks are at  $1637$ ,  $1531$ ,  $1415$ ,  $1328$ ,  $1166$ ,  $1091$ ,  $853$ ,  $752$ ,  $701$ ,  $624$ , and  $565\text{ cm}^{-1}$ . Several differences are evident when comparing the *E. coli* and *P. aeruginosa* spectra in Figs. 1 and 2. In particular, the peaks at  $1539$ ,  $1283$ ,  $1240$ ,  $1057$  and  $956$ , and  $813\text{ cm}^{-1}$  in the *E. coli* spectra are either not present or are much reduced in the *P. aeruginosa* spectra, the dominant *E. coli* peak at  $1354\text{ cm}^{-1}$  is a double peak in the *P. aeruginosa* spectra (i.e., there is also a peak at  $1328\text{ cm}^{-1}$ ), the *P. aeruginosa* peaks at  $540$  and  $1091\text{ cm}^{-1}$  do not appear in the *E. coli* spectra, and several peaks (at  $624$ ,  $1166$ , and  $1283\text{ cm}^{-1}$ ) are noticeably enhanced in the *P. aeruginosa* spectra relative to the *E. coli* spectra.

Our spectra for *E. coli* compare well with recent results (also at  $514.5\text{ nm}$  laser excitation) obtained by Zeiri et al.,<sup>41</sup> who used a different method of coating the bacteria with silver colloid. In their study, bacteria act as nucleation centers for the silver colloid formation and are introduced during the preparation of the colloids, whereas

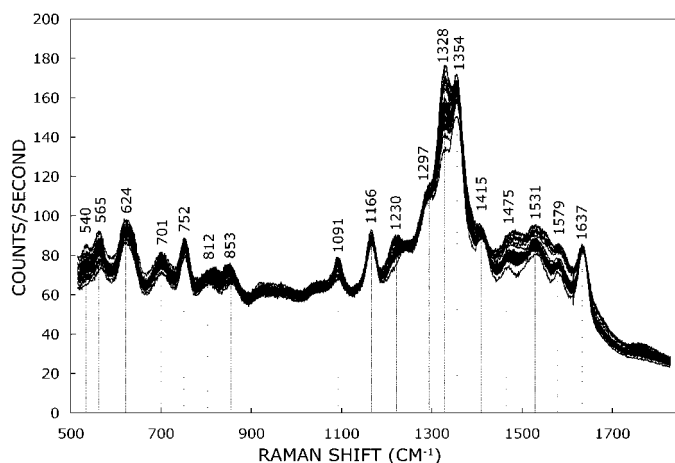


Fig. 2. Twenty-four SERS spectra of *P. aeruginosa* bacteria, with VR equal to 50:1 (Ag colloid solution to bacterial suspension) for all spectra. Spectra are normalized such that the Raman water peaks are at the same height for all scans. The variation (maximum = 25%, average ~15%) between spectra gives an indication of experimental reproducibility, as well as the variability due to aggregation of the colloid particles over a 4-h period.

in our method the silver colloid is made first and later mixed with the bacteria. Although Zeiri et al.<sup>41</sup> find some evidence that different parts of the cell give different spectra, their spectra appear to be dominated by a flavin adenine dinucleotide (FAD)-like compound present in the plasma membrane of the cell. We also observe this same FAD compound that dominates their bacterial spectra.

We also find several spectral features that are different from those present in Fig. 8 in Zeiri et al.<sup>41</sup> For instance, the peaks we observe at  $956$  and  $1240\text{ cm}^{-1}$  are not present in any of their data, our peak at  $753\text{ cm}^{-1}$  is much larger than the one they observe (although their peak at  $550\text{ cm}^{-1}$  is much larger than the one we observe), and they observe peaks at  $850$  and  $1080\text{ cm}^{-1}$  that are not present in our data.

Some of the differences between our data and that of Zeiri et al.<sup>41</sup> may be due to different methods of sample preparation and measurement. Our bacteria are mixed with the already-prepared silver colloid solution, and we obtain spectra from aqueous mixtures in glass cuvettes instead of dry samples on a glass slide. Because our *E. coli* and *P. aeruginosa* samples are suspended in deionized water for up to one day before measurement, the cell walls may be rupturing so that we are seeing other components of the cell in the aqueous mixture. Although we have no independent evidence for this, it is possible that the PAMB bacteria are not rupturing because they are suspended in artificial seawater (a medium similar to that in which they live). In this case, our results would be complicated by comparing components of the wall in one case (PAMB bacteria), and of the whole cell in the other (*E. coli* and *P. aeruginosa*).

**Methods and Reproducibility of Spectra.** We obtained spectra from suspensions of both deionized water and artificial seawater mixed with silver colloid to check that we were not observing features of the aqueous suspensions in the SERS spectra.<sup>1</sup> We found that a deionized water/silver colloid spectrum is identical to the Raman spectrum for pure water with a peak at  $1637\text{ cm}^{-1}$ . The

artificial seawater/silver colloid (100:1, Ag col:ASW) spectrum exhibits some broad fluorescence in the range 1100–1500  $\text{cm}^{-1}$ , but no distinct peaks except the 1637  $\text{cm}^{-1}$  water Raman peak. Therefore, we are confident that the aqueous suspensions add no spectral peaks (except the identifiable water peak) to the SERS spectra of the bacteria.

We studied the reproducibility of *P. aeruginosa* SERS spectra by examining 24 spectra taken over a 4-h period. In Fig. 2, all of the spectra have been divided by the integration time, then normalized so that the Raman water peak at 1637  $\text{cm}^{-1}$  is the same height, to within 3%. The spectra are shifted so that the water peaks (at 1637  $\text{cm}^{-1}$ ) lie on top of each other. (This is the same analysis as used in Fig. 1). With this normalization it is clear that there are many peaks in the spectrum that change less than 20% during colloidal aggregation (624, 701, 752, 853, 1091, 1166, 1354, 1415, and 1637  $\text{cm}^{-1}$ ). The peaks at 752, 1166, and 1637  $\text{cm}^{-1}$  change by less than 10%. Note that the background level between 850 and 1300  $\text{cm}^{-1}$  also appears to change by less than 10%. On the other hand, there are also regions in the spectrum that are quite sensitive to colloidal aggregation effects, such as between 500 and 600  $\text{cm}^{-1}$  and between 1400 and 1600  $\text{cm}^{-1}$ , where the background changes by as much as 25%.

We have observed aggregation of colloidal particles induced by *E. coli* bacteria over a time period of one day,<sup>40</sup> and so we expect that some colloidal aggregation will occur over the 4-h time period. Because this aggregation will affect the intensity of the peaks, the variability we measured is an upper limit on experimental errors, combining both experimental error and sample variability.

We also observed that aggregation effects are much more pronounced in the PAMB/colloidal suspensions than in the MTAB/colloidal suspensions. There is evidence<sup>42</sup> that the  $\text{Cl}^-$  ions in the artificial seawater induce rapid colloid aggregation. When we measured PAMB spectra we found it was necessary to obtain the spectra immediately after mixing the PAMB solution and colloidal suspension; otherwise, it was evident that aggregation had occurred (black precipitate was observed). Because aggregation was occurring so rapidly, it was difficult to optimize the SERS signal intensity, unlike for MTAB. This is the reason that the PAMB SERS spectra appear noisier than the MTAB SERS spectra.

Given that the PAMB/colloidal solutions were much less stable than the MTAB/colloidal solutions, the reproducibility of the *P. aeruginosa* SERS spectra should be taken to be representative of MTAB SERS spectra, but only representative of PAMB SERS spectra if measurements are made within 5–10 min of mixing the colloidal suspension and the PAMB solution (as in our methodology).

We observed very little deterioration of the bacterial solutions (bacteria plus water) over a time period less than one day (the maximum amount of time we used the bacterial solution before using a newly grown solution). In Fig. 3, the spectrum at  $t = 0$  was taken from a freshly prepared colloidal solution (<20 min old) mixed with freshly grown 6M3 bacteria (<1 h old). The second spectrum ( $t < 1$  day) was taken using the same bacterial solution, which was now almost a day old, mixed with a

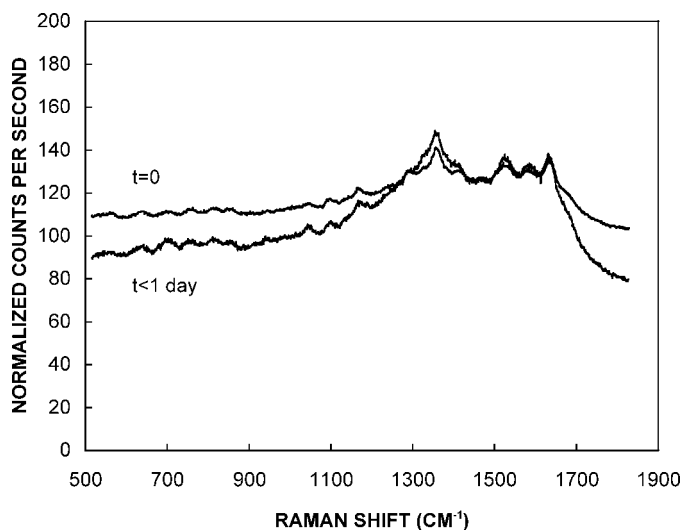


FIG. 3. Comparison of a 6M3 bacterial solution over a time period of less than one day. The  $t = 0$  solution was a mixture of a fresh bacterial solution (<1 h) with fresh colloidal suspension (<20 min). The  $t < 1$  day solution was a mixture of the same bacterial solution, about a day later, mixed again with a freshly made colloidal suspension. There is no more than 23% variation between the two spectra for any Raman shift, and the average variation is 9%. The fact that the peaks seen in the two spectra have not changed indicates that the bacteria does not change or deteriorate in a time period of less than a day. The background differences may be due to differences in the colloid suspension.

freshly made colloidal suspension. The data have been normalized to the water peak height and shifted so that the water peaks lie on top of each other. The % difference, (absolute value  $(I(t_1) - I(t_2))/I(t_1) * 100$ ), for the two spectra has a maximum of 23%, but an average value of 9% over the spectral range 515–1827  $\text{cm}^{-1}$ .

**PAMB Spectra Compared to *E. coli* and *P. aeruginosa*.** Figure 4 shows the SERS spectra from *E. coli* and *P. aeruginosa* (MTAB) and marine bacterial strains 34H, 6M3, 6M4, 6B1, and 11B5 (PAMB). Each PAMB spectrum shown in Fig. 4 is an average of at least seven spectra. For Fig. 4, first we normalized the water background (either pure deionized water or artificial seawater, depending on the bacteria) to the bacteria spectra (at 1827  $\text{cm}^{-1}$ ) and then subtracted the water background from the averaged bacteria spectrum. The water backgrounds were obtained using an Ag colloid solution and are displayed in Fig. 5.

The silver colloid/PAMB spectra contain dominant peaks at 1361, 1635, 1533, 1587, 1293, 1174, 1053, 759, and 705  $\text{cm}^{-1}$ . There is an indication of a peak in all the PAMB spectra at 1135  $\text{cm}^{-1}$  that does not occur in the *E. coli* and *P. aeruginosa* spectra. The five PAMB spectra are quite similar to each other. The positions of the major peaks occur at similar Raman shifts, with only small differences in peak height. However, the PAMB spectra are clearly different from the *E. coli* and *P. aeruginosa* spectra in several aspects, in particular, in the regions 900–1300  $\text{cm}^{-1}$  and 500–700  $\text{cm}^{-1}$ .

In Fig. 4, lines are drawn centered on the PAMB peaks so that differences can clearly be seen with the MTAB spectra. The large peak in the PA01 spectra at 624  $\text{cm}^{-1}$  is shifted significantly from the small peak at 646  $\text{cm}^{-1}$  in the PAMB spectra. Other peaks at 759 and 573  $\text{cm}^{-1}$  are not noticeably shifted, but the relative amplitudes are

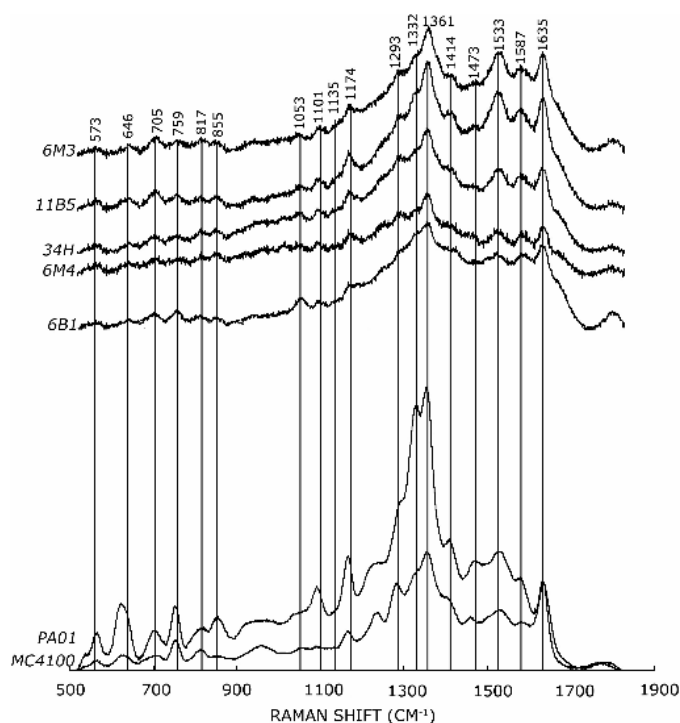


FIG. 4. Comparison of five strains of Arctic psychro-active marine bacteria (6B1, 6M4, 6M3, 34H, and 11B5) with *P. aeruginosa* (PA01) and *E. coli* (MC4100) spectra. The lines and Raman shift numbers are positioned on the 34H peaks. After the artificial seawater baseline spectrum was subtracted from the PAMB spectra and the deionized water baseline spectrum was subtracted from the MTAB spectra, the resulting spectra have been shifted for ease of viewing. The MTAB spectra are averages of up to 13 spectra.

different. The relative intensities of peaks in the region 570–900  $\text{cm}^{-1}$  are similar for all of the PAMB, but are not similar to the peaks of either PA01 or MC4100.

The ratio of the height of the 1053  $\text{cm}^{-1}$  peak to the 1101  $\text{cm}^{-1}$  peak is larger for the PAMB spectra than for the PA01 and MC4100 spectra. Also for PA01, the dom-

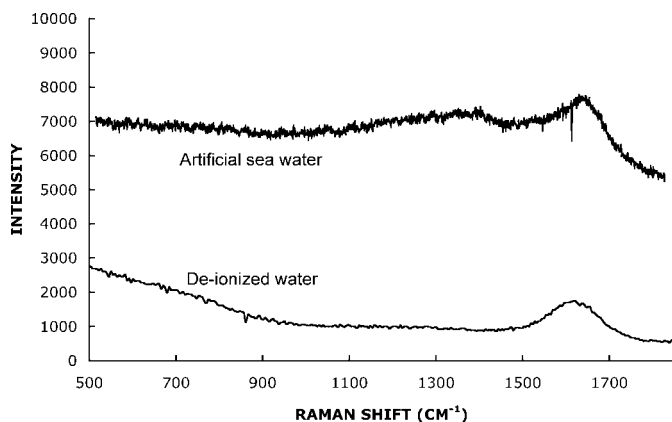


FIG. 5. SERS spectra of artificial seawater and pure deionized water. The artificial seawater spectra was subtracted from the PAMB spectra and the deionized water spectra was subtracted from the PA01 and MC4100 spectra to obtain the spectra shown in Fig. 4.

inant peak at 1361  $\text{cm}^{-1}$  is a narrow, double peak with several obvious shoulder peaks at 1293, 1414, and 1250  $\text{cm}^{-1}$ , whereas for the PAMB, it is a single broad peak with shoulder peaks at 1293, 1332, and 1414  $\text{cm}^{-1}$ , but not at 1250  $\text{cm}^{-1}$ . The MC4100 spectrum is similar to the PA01 spectrum near the 1361  $\text{cm}^{-1}$  peak, but is not double-peaked.

The peaks in the region between 1400 and 1650  $\text{cm}^{-1}$  for the PAMB spectra are almost as large as the dominant peak at 1361  $\text{cm}^{-1}$  and are distinct, whereas there appears to be one broad peak with shoulders centered at 1553  $\text{cm}^{-1}$  in the PA01 and MC4100 spectra.

The differences between spectra of the MTAB and PAMB species are the largest reported so far for bacterial samples. Using SERS, these species are easily distinguishable without resorting to multivariate analysis of the data.

**Peak Identification.** Table I shows our tentative assignment of the peaks seen in the SERS spectra of *E.*

TABLE I. Assignment of the peaks ( $\text{cm}^{-1}$ ) for the average SERS spectra for *C. psychrerythraea*, str. 34H, *E. coli*, and *P. aeruginosa*. (Notation: b = broad, m = medium, s = strong, sh = shoulder, vw = very weak, w = weak.)

MC4100 <i>E. coli</i>	PA01 <i>P. aeruginosa</i>	34H <i>C. psychrerythraea</i>	Tentative peak assignment
	540(w)		
571(m)	565(s)	573(m)	carbohydrates <sup>39</sup>
636(s)	624(s)	646(m)	COO <sup>-</sup> bend <sup>44</sup>
703(m)	701(w)	705(m)	adenine from flavin <sup>47</sup>
753(s)	752(w)	759(m)	ring I deformation <sup>45</sup>
813(m), 853(vw)	812(m), 853(m)	817(w), 855(w)	different C–N stretch, <sup>46–47</sup> probably from tyrosine groups <sup>47</sup>
964(s,b)			C–N stretch <sup>47</sup>
1057(w), 1089(w)	1091(m)	1053(m), 1101(s)	carbohydrates, C–C, C–O, –C– OH deformation <sup>46</sup>
		1135(w)	=C–C= unsaturated fatty acids in lipids, C–N (protein) <sup>46,48</sup>
1166(m)	1166(s)	1174(m)	aromatic amino acids in proteins <sup>48</sup>
1240(m, sh)	1250(m, sh)		N–H, C–N, amide III <sup>46</sup>
1283(m)	1297(s)	1293(m, sh)	=CH in plane (lipid) or amide III (protein) <sup>48</sup>
1355(s)	1328(m, sh), 1354(s)	1332(sh), 1361(s)	C–H bend (protein) <sup>48</sup>
1404(s, sh)	1415(w, sh)	1414(w, sh)	COO <sup>-</sup> symmetric stretch <sup>47</sup>
1460(w)	1475(w, sh)	1473(w)	CH <sub>2</sub> bend (protein, lipid) <sup>48</sup>
1539(s, b)	1531(s)	1533(s)	N–H, C–H bend, C=C stretch <sup>45</sup>
1587(w)	1579(w)	1587(m)	C=C (lipid) <sup>46</sup>
1635(s)	1637(s)	1635(s)	amide I, <sup>44</sup> water

*coli*, *P. aeruginosa*, and PAMB strain 34H. The small peak at 1135 cm<sup>-1</sup> in the PAMB spectra that is missing in the MTAB spectra has been attributed to the =C–C= in the unsaturated fatty acids in lipids.<sup>43</sup> Peaks in the 500–1100 cm<sup>-1</sup> region are due to various groups including glycosides, nucleic acids (cytidine, uracil), proteins (tyrosine), phenylalanine, carbohydrates, and unsaturated fatty acid and lipids that are present in the bacterial cell.<sup>44</sup>

The major SERS peaks at 1361 cm<sup>-1</sup>, 1293 cm<sup>-1</sup>, 1250 cm<sup>-1</sup>, 1174 cm<sup>-1</sup>, and 1533 cm<sup>-1</sup> are the characteristic peaks seen in the amino acids L-lysine, D-glutamic acid, D-alanine, and N-acetyl glucosamine, as discussed in detail in Sengupta et al.<sup>1</sup> We have identified these peaks as being due to various bends and stretches of proteins as shown in Table I, according to the references cited there.

The 759 cm<sup>-1</sup> peak is more intense in the *P. aeruginosa* and *E. coli* spectra than in the PAMB spectra. This peak has been attributed to polysaccharide structures such as peptidoglycan, which is made up of N-acetyl-D-glucosamine (NAG) and N-acetylmuramic acid,<sup>35</sup> and also ring I deformation of reduced FAD.<sup>45</sup>

The peak at 1635 cm<sup>-1</sup> is an amide peak for spectra where the water background has been subtracted. In those spectra (Figs. 1–3) without the water background subtracted, the water Raman peak overlays the amide peak.

**Cold Adaptation.** The spectral differences between *E. coli* and *P. aeruginosa* and PAMB could be a direct result of differences in the fatty acid composition of the PAMB cell membranes. It has been found that cold-adapted bacteria alter the fatty acid composition of their cell membranes by increasing the amount of unsaturation of the fatty acids, shortening the fatty acid chain lengths, or increasing the number of methyl-branched-chain fatty acids.<sup>46</sup>

The presence of the small 1135 cm<sup>-1</sup> peak (identified as due to unsaturated fatty acids in lipids) in the PAMB spectra is consistent with observations of the presence of PUFAs in the membranes of closely related bacterial strains. This also provides support for the claim that cold adaptation in PAMB (via membrane fluidity) is assisted by the production of poly-unsaturated fatty acids within their cell membranes.<sup>15,20,46</sup>

## CONCLUSION

In this paper we have presented a preliminary attempt to characterize the outer cell membrane surfaces of psychro-active marine bacteria using SERS. We find that we cannot distinguish between the PAMB strains to within our measured experimental reproducibility, but we find differences (greater than our experimental reproducibility) between the MTAB and the PAMB. Differences in the outer cell surface constituents (particularly the lipid composition of their membranes) of psychro-active and mesophilic bacteria may explain the differences in their SERS spectra.

Several mechanisms have been proposed to explain cold adaptation in sea-ice bacteria, including attachment to surfaces, protein folding, polyunsaturated fatty acid synthesis, and psychro-active extra-cellular enzyme production. Our results lend support to the observation that psychro-active bacteria contain unsaturated fatty acids in their outer cell membranes. We see significant differences

both in the 400–980 cm<sup>-1</sup> region and in the region from 980–1600 cm<sup>-1</sup>. In particular, the indication of a peak at 1135 cm<sup>-1</sup> in the PAMB spectra suggests that there may be PUFAs present in the PAMB that are not present in the MTAB.

Several independent studies suggest that psychro-active bacteria have different bio-molecular structures in their cell membrane walls from mesophilic bacteria, due to evolving in and adapting to continuously cold environments. This work suggests that SERS may be a useful technique for distinguishing and fingerprinting bacteria that are found in distinctly different environments and can be used to examine specific biochemical differences among bacteria.

## ACKNOWLEDGMENTS

The authors would like to thank Professors Daniel T. Schwartz and François Baneyx for their interest and advice, and Mirna Mujacic for providing the *E. coli* and *P. aeruginosa* bacterial samples. Support for this research was provided by the National Science Foundation Grants CTS-9982413 and ATM-0323930, the Office of Polar Programs Grant OPP-0338333, the University of Washington/PNNL Joint Institute for Nanotechnology, and the University of Washington Center for Nanotechnology.

1. A. Sengupta, M. L. Laucks, N. Dildine, E. Darpala, and E. J. Davis, *J. Aerosol Sci.* **36**, 651 (2005).
2. J. P. Bowman, *Adv. Microb. Ecol.*, paper in press (2004).
3. J. T. Staley and J. J. Gosink, *Annu. Rev. Microbiol.* **53**, 189 (1999).
4. R. Y. Morita, *Bacteriol. Rev.* **39**, 144 (1975).
5. K. Junge, J. F. Imhoff, J. T. Staley, and J. W. Deming, *Microb. Ecol.* **43**, 315 (2002).
6. A. L. Huston, B. B. Krieger-Brockett, and J. W. Deming, *Environ. Microbiol.* **2**, 383 (2000).
7. J. W. Deming, *Curr. Opin. Microbiol.* **3**, 301 (2002).
8. K. Junge, H. Eicken, and J. W. Deming, *Appl. Environ. Microbiol.* **69**, 4282 (2003).
9. J. P. Bowman, J. J. Gosink, S. A. McCammon, T. E. Lewis, D. S. Nichols, P. D. Nichols, J. H. Skerrat, J. T. Staley, and T. A. McMeekin, *Int. J. Syst. Bacteriol.* **48**, 1171 (1998).
10. J. W. Deming and K. Junge, "Colwellia", in *The Proteobacteria, Part B, Bergey's Manual of Systematic Bacteriology*, G. T. Staley, D. J. Benner, N. R. Krieg, and G. M. Garrity, Eds. (Springer, New York, 2005), 2nd ed., Vol. 2, pp. 447–454.
11. D. N. Thomas and G. S. Dieckmann, *Science* (Washington, D.C.) **295**, 641 (2002).
12. J. T. Staley, K. Junge, and J. Deming, "And some like it cold: sea ice microbiology", in *Biodiversity of Life*, J. T. Staley and A.-L. Reysenbach, Eds. (Wiley-Liss, Inc., New York, 2002), pp. 423–438.
13. E. Helmke and H. Weyland, *Mar. Ecol. Prog. Ser.* **117**, 269 (1995).
14. K. Junge, H. Eicken, and J. W. Deming, *Appl. Environ. Microbiol.* **70**, 550 (2004).
15. D. S. Nichols, J. Bowman, K. Sanderson, C. M. Nichols, T. Lewis, T. McMeekin, and P. D. Nichols, *Curr. Opin. Biotechnol.* **10**, 240 (1999a).
16. D. S. Nichols, A. R. Greenhill, C. T. Shabolt, T. Ross, and T. A. McMeekin, *Appl. Environ. Microbiol.* **65**, 3757 (1999b).
17. D. S. Nichols, J. Olley, H. Garda, R. R. Brenner, and T. McMeekin, *Appl. Environ. Microbiol.* **66**, 2422 (2000).
18. N. J. C. Fong, M. L. Burgess, K. D. Barrow, and D. R. Glenn, *Appl. Microbiol. Biotechnol.* **56**, 750 (2001).
19. M. K. Chattopadhyay and M. V. Jagannadham, *Polar Biol.* **24**, 386 (2001).
20. N. J. Russell and D. S. Nichols, *Microbiology* **145**, 767 (1999).
21. M. Fleischmann, P. J. Hendra, and A. J. McQuillan, *Chem. Phys. Lett.* **26**, 163 (1974).
22. K. H. Kneipp, I. Itzkan, R. R. Dasari, and M. Feld, *J. Phys.: Condens. Matter* **14**, R597 (2002).
23. C. D. Keating, K. K. Kovaleski, and M. J. Natan, *J. Phys. Chem. B.* **102**, 9414 (1998).
24. S. Lefrant, J. P. Buisson, J. Schreiber, O. Chauvet, M. Baibarac, and I. Baltog, *Synth. Met.* **139**, 783 (2003).

25. M. Kerker, D. S. Wang, H. Chew, O. Siiman, and L. A. Bumm, in *Surface Enhanced Raman Scattering*, R. K. Chang and T. E. Furtak, Eds. (Plenum Press, New York, 1982), 1st ed., Vol. 1, p. 109.
26. M. Moscovits, *Rev. Mod. Phys.* **57**, 783 (1985).
27. G. D. Sockalingum, H. Lamfarraj, P. Pina, A. Beljebbar, P. Allouch, and M. Manfait, *Eur. J. Histochem.* **43**, Suppl. 1, 39 (1999).
28. K. C. Schuster, I. Reese, E. Urlaub, J. R. Gapes, and B. Lendl, *Anal. Chem.* **72**, 5529 (2000).
29. S. Farqharson, A. D. Gift, P. Maksymiuk, and F. E. Inscore, *Appl. Spectrosc.* **58**, 351 (2004).
30. L. A. Gearheart, H. J. Ploehn, and C. J. Murphy, *J. Phys. Chem. B* **105**, 12609 (2001).
31. E. Podstawka, Y. Ozaki, and L. M. Proniewicz, *Appl. Spectrosc.* **58**, 570 (2004).
32. E. Podstawka, Y. Ozaki, and L. M. Proniewicz, *Appl. Spectrosc.* **58**, 581 (2004).
33. E. Podstawka, Y. Ozaki, and L. M. Proniewicz, *Appl. Spectrosc.* **58**, 1147 (2004).
34. L. Zeiri, B. V. Bronk, Y. Shabtai, J. Czege, and S. Efrima, *Colloids and Surfaces A* **208**, 357 (2002).
35. R. M. Jarvis and R. Goodacre, *Anal. Chem.* **76**, 40 (2004).
36. R. Keir, E. Igata, M. Arundell, W. E. Smith, D. Graham, C. McHugh, and J. M. Cooper, *Anal. Chem.* **74**, 1503 (2002).
37. C. H. Munro, W. E. Smith, M. Garner, J. Clarkson, and P. C. White, *Langmuir* **11**, 3712 (1995).
38. P. C. Lee and D. Meisel, *J. Phys. Chem.* **86**, 3391 (1982).
39. R. Keir, D. Sadler, and W. E. Smith, *Appl. Spectrosc.* **56**, 551 (2002).
40. A. Sengupta, M. L. Laucks, and E. J. Davis, *Appl. Spectrosc.* **59**, 1016 (2005).
41. L. Zeiri, B. V. Bronk, Y. Shabtai, J. Eichler, and S. Efrima, *Appl. Spectrosc.* **58**, 33 (2004).
42. W. Xu, S. Xu, Z. Lu, L. Chen, B. Zhao, and Y. Ozaki, *Appl. Spectrosc.* **58**, 414 (2004).
43. K. C. Schuster, E. Urlaub, and J. R. Gapes, *J. Microbiol. Methods* **42**, 29 (2000).
44. K. C. Schuster, I. Reese, E. Urlaub, J. R. Gapes, and B. Lendl, *Anal. Chem.* **72**, 5529 (2000).
45. Y. Zheng, P. R. Carey, and B. A. Palfey, *J. Raman Spectrosc.* **35**, 521 (2004).
46. D. S. Nichols, P. D. Nichols, and T. A. McMeekin, *Sci. Prog.* **78**, 311 (1995).
47. H. Zhao, B. Yuan, and X. Dou, *J. Opt. A: Pure Appl. Opt.* **6**, 900 (2004).
48. K. Venkatakrishna, J. Kurien, K. M. Pai, M. Valiathan, N. N. Kumar, C. M. Krishna, G. Ullas, and V. B. Kartha, *Curr. Sci.* **80**, 665 (2001).